A hierarchy of particle-size segregation models: From polydisperse mixtures to depth-averaged theories

J. M.N.T. Gray

Citation: AIP Conf. Proc. **1542**, 66 (2013); doi: 10.1063/1.4811869
View online: http://dx.doi.org/10.1063/1.4811869
View Table of Contents: http://proceedings.aip.org/dbt/dbt.jsp?KEY=APCPCS&Volume=1542&Issue=1
Published by the AIP Publishing LLC.

A hierarchy of particle-size segregation models: From polydisperse mixtures to depth-averaged theories

J.M.N.T. Gray

School of Mathematics and Manchester Centre for Nonlinear Dynamics, The University of Manchester, Oxford Road, Manchester, M13 9PL, UK

Abstract.
Particle size segregation in granular avalanches occurs due to inter-particle percolation and squeeze expulsion. The general theory for a polydisperse mixture yields a segregation equation for each grain size class. For a three constituent mixture of large, small and medium sized particles there are three segregation equations, one of which can be eliminated, since the concentrations of all the species necessarily sums to unity. The remaining two coupled parabolic equations can be solved using a standard Galerkin finite element method. Numerical solutions show that small particles percolate to the base of the avalanche, large particles are squeezed to the surface and the medium sized grains are sandwiched in between. For certain choices of the segregation parameters it is possible to generate instabilities that lead to saw-tooth segregation in the three-phase mixture, but these die off as the grains separate into bi-disperse sub-mixtures. In general, all the grains contribute to the segregation process and develop an inversely graded particle size distribution, that coarsens upwards. This is known as *reverse distribution grading*. Sometimes, however, the fine particles may not segregate readily, leading to *reverse coarse tail grading*. For a bi-disperse mixture, the general theory yields one independent segregation equation, which always seeks to drive the particles into an inversely graded state. However, when the bulk flow shears small particles over the top of large, a *breaking size-segregation wave* is created. Such waves are important close to flow fronts, because they allow large particles that are over-run to rise up to the surface again and be recirculated. Computing the evolving particle-size distribution in a three-dimensional flow is still a challenge. However, it is possible to obtain a simplified representation by integrating the segregation equation through the avalanche depth. This fits naturally into the depth-averaged framework of avalanche models and opens the door to fully couple calculations to study levee formation and segregation induced flow fingering.

Keywords: Granular avalanches, segregation, mixing, pattern formation, shock waves
PACS: 45.70.Ht, 45.70.Mg, 45.70.Qj, 47.40.Nm, 89.75.Kd

Introduction

Poly-disperse granular materials are extremely common in our kitchens, in our natural environment, as well as in many industrial, pharmaceutical, chemical and agricultural processes. Particles rarely have a regular shape or a uniform size distribution, and it is technologically challenging and costly to produce high tolerance monodisperse spheres. As polydisperse granular materials are moved, stored, agitated or allowed to flow, they have a tendency to segregate. This can sometimes be desirable, such as in mining and stone crushing, and can be exploited to separate the grains [1], but it is often a source of great frustration that can significantly degrade the quality and the safety of a product [2]. A considerable amount of early work was therefore performed by engineers who sought to understand the fundamental size segregation mechanisms and learn how to control their effects [3, 4, 5]. Geologists and sedimentologists were also early pioneers who were quick to identify inversely (or reverse) graded deposits, in which the grain size population coarsens upwards, and use this as an indicator of ancient granular avalanches on dunes, in dense pyroclastic flows and debris flows [e.g. 6, 7]. As many as thirteen different segregation mechanisms for dissimilar grains have now been identified [8], with the primary ones being percolation [e.g. 7, 9], trajectory segregation [e.g. 10], convection [e.g. 11] and fluidization [e.g 12].

In shallow granular avalanches it is widely accepted that void filling percolation is the dominant mechanism for size segregation [13, 14]. This is the process in which random fluctuations within the flowing avalanche constantly open up gaps and the smaller particles are statistically more likely to drop down into them, under the action of gravity, than the large ones, because they are more likely to fit into the available space. This void filling process has also been termed kinetic sieving [7] and there is a related process of squeeze expulsion, in which large particles are levered upwards [13]. This percolation mechanism is extremely efficient in dry granular flows, with the large ones rising to the surface even when there are only small size differences between the particles, and when the large particles are significantly denser than the small ones [15].

Even over short distances particle segregation can have a significant impact as shown in the rotating drum experiment in figure 1. A single passage through the surface avalanche is sufficient to sort the grains and deposit

Powders and Grains 2013
AIP Conf. Proc. 1542, 66-73 (2013); doi: 10.1063/1.4811869

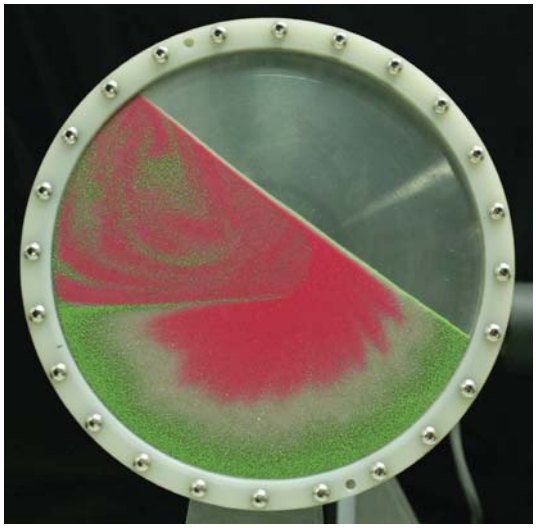

FIGURE 1. Segregation of a three phase mixture composed of 500-750 μm (green), 400-500 μm (white) and 75-150 μm (pink) particles in a rotating drum. The segregation occurs in a thin surface avalanche, and there is no segregation while the grains are in slow solid body rotation. The homogeneous initial condition is still visible in the top left, but once the grains have passed through the avalanche and been deposited they form a radial pattern [copyright Cambridge University Press 2011 reprinted with permission 16].

them to form a radial segregation pattern, with large particles concentrated near the drum wall, small ones near the centre and medium ones in between. A close-up image of the surface avalanche and the segregation within it is shown in figure 2.

Derivation of the segregation equations

Consider a polydisperse mixture of particles of the same density, but with differing sizes, that flows down a chute inclined at an angle ζ to the horizontal. A coordinate system $Oxyz$ is defined with the x-axis pointing down the chute, the y-axis pointing across the chute and the z-axis being the upward pointing normal. For each constituent ν, mixture theory [17, 18] defines overlapping partial densities, ρ^ν, partial velocities, $\mathbf{u}^\nu$, and partial pressures, p^ν. In addition, the concentration, ϕ^ν, is defined as the volume fraction of constituent ν per unit volume of mixture, and lies in the range

$$0 \leq \phi^\nu \leq 1. \tag{1}$$

The sum over all constituents is necessarily equal to unity

$$\sum_{\forall \nu} \phi^\nu = 1. \tag{2}$$

In standard mixture theory the partial and intrinsic velocity fields are identical, but the other fields such as the density, Cauchy stresses and pressures are usually related by a linear volume fraction scaling

$$\rho^\nu = \phi^\nu \rho^{\nu *}, \quad \mathbf{T}^\nu = \phi^\nu \mathbf{T}^{\nu *}, \quad p^\nu = \phi^\nu p^{\nu *}, \quad \mathbf{u}^\nu = \mathbf{u}^{\nu *}. \tag{3}$$

The bulk density ρ and the bulk pressure p are defined as the sum of the partial densities and partial pressures

$$\rho = \sum_{\forall \nu} \rho^\nu, \quad p = \sum_{\forall \nu} p^\nu. \tag{4}$$

Each constituent satisfies individual mass

$$\frac{\partial \rho^\nu}{\partial t} + \nabla \cdot (\rho^\nu \mathbf{u}^\nu) = 0, \tag{5}$$

and momentum

$$\frac{\partial}{\partial t}(\rho^\nu \mathbf{u}^\nu) + \nabla \cdot (\rho^\nu \mathbf{u}^\nu \otimes \mathbf{u}^\nu) = \nabla \cdot \mathbf{T}^\nu + \rho^\nu \mathbf{g} + \mathbf{b}^\nu, \tag{6}$$

balance laws, where $\otimes$ is the dyadic product and $\mathbf{g}$ is the gravitational acceleration vector. The interaction force, $\mathbf{b}^\nu$, is the force exerted on phase ν by all the other constituents. These interaction forces sum to zero over all constituents

$$\sum_{\forall \nu} \mathbf{b}^\nu = \mathbf{0}. \tag{7}$$

The stress tensor $\mathbf{T}^\nu = -p^\nu \mathbf{1} + \mathbf{s}^\nu$ is broken down into a spherical pressure $-p^\nu \mathbf{1}$ and a deviatoric stress $\mathbf{s}^\nu$, where $\mathbf{1}$ is the unit tensor. It is assumed that in the normal direction the pressure dominates, and the deviatoric stresses and the normal acceleration terms can be neglected. This implies that the normal components of the momentum balances (6) sum to

$$\frac{\partial p}{\partial z} = -\rho g \cos\zeta, \tag{8}$$

over all constituents, where g is the constant of gravitational acceleration. Since the bulk density is constant and the avalanche free-surface, at $z = s(x,y,t)$, is traction free, equation (8) can be integrated through the avalanche depth, subject to the condition that $p(s) = 0$, to show that the pressure is lithostatic

$$p = \rho g (s - z) \cos\zeta. \tag{9}$$

Gray and Thornton [19] observed that small particles support less of the overburden pressure as they percolate downwards, and that the large grains must consequently support more of the load. This led them to introduce a factor, f^ν, which determines the proportion of the lithostatic pressure carried by constituent, ν, i.e.

$$p^\nu = f^\nu p. \tag{10}$$

FIGURE 2. Close up photograph of the segregation within the surface avalanche in the thin rotating drum experiment shown in figure 1. The avalanche rapidly develops an inversely graded particle size distribution, with the large green particles on top, the small pink particles at the bottom and the medium sized white grains sandwiched in between [copyright Cambridge University Press 2011 reprinted with permission 16].

Summing the partial pressure (10) over all constituents and using (4) implies that the f^ν factors must sum to unity

$$\sum_{\forall \nu} f^\nu = 1. \tag{11}$$

We shall adopt the same form for the interaction drag law, $\mathbf{b}^\nu$, proposed by [20], which consists of three terms

$$\mathbf{b}^\nu = p\nabla f^\nu - \rho^\nu c(\mathbf{u}^\nu - \mathbf{u}) - \rho d\nabla\phi^\nu, \tag{12}$$

where c is the coefficient of inter-particle drag, d is the coefficient of diffusive remixing and $\mathbf{u}$ is the barycentric or bulk velocity, defined by

$$\rho\mathbf{u} = \sum_{\forall \nu} \rho^\nu \mathbf{u}^\nu. \tag{13}$$

The first term in (12) combines with the pressure gradient in (6) to ensure that the percolation process is driven by the intrinsic rather than the partial pressure gradient, the second provides a linear resistance to relative motion and the third models diffusive remixing of the particles. The interaction drag $\mathbf{b}^\nu$ has been constructed so that it automatically satisfies the summation condition (7).

The bulk velocity $\mathbf{u}$ has components u, v and w in the downslope, cross slope and normal directions, respectively. In the down and cross-slope directions the constituent velocities, u^ν and v^ν, are assumed to be equal to the bulk velocity

$$u^\nu = u, \quad v^\nu = v. \tag{14}$$

While the constituent velocity components in the normal direction can be calculated by substituting (3), (8), (10) and (12) into the normal component of the momentum balance (6). Assuming that the normal accelerations are negligible, this implies that

$$\phi^\nu w^\nu = \phi^\nu w + (f^\nu - \phi^\nu)(g/c)\cos\zeta - (d/c)\frac{\partial\phi^\nu}{\partial z}. \tag{15}$$

The functions f^ν determine whether a particle will rise ($f^\nu > \phi^\nu$) or sink ($f^\nu < \phi^\nu$) relative to bulk, and must satisfy two constraints. Firstly if the any class of particles are in a pure phase they carry all of the load

$$f^\nu = 1, \quad \text{when} \quad \phi^\nu = 1, \tag{16}$$

and secondly, when there are no particles of that phase, they cannot carry any of the load

$$f^\nu = 0, \quad \text{when} \quad \phi^\nu = 0. \tag{17}$$

Motivated by the case of segregation in bi-disperse mixtures Gray and Ancey [16] proposed that in a polydisperse mixture

$$f^\nu = \phi^\nu + \sum_{\forall \mu} B_{\nu\mu}\phi^\nu\phi^\mu, \tag{18}$$

where the non-dimensional parameter $B_{\nu\mu}$ determines the magnitude of the pressure perturbation for constituent ν due to the presence of constituent μ. This additive decomposition automatically satisfies the constraints (16) and (17), and reduces to the bi-disperse case in any two-component sub-mixture. Assuming that there are no pressure perturbations exerted by any constituent on itself

$$B_{(\nu\nu)} = 0, \quad \forall\nu, \tag{19}$$

and the pressure perturbation on constituent ν due to constituent μ is equal and opposite to the pressure perturbation on constituent μ by constituent ν

$$B_{\nu\mu} = -B_{\mu\nu}, \quad \forall\nu \neq \mu, \tag{20}$$

then the summation condition (11) is automatically satisfied as well. The matrix $\mathbf{B}$ formed by the coefficients $B_{\nu\mu}$ has the interesting property that it is antisymmetric, i.e. $\mathbf{B} = -\mathbf{B}^T$, where the superscript T denotes the transpose.

An equation for the normal velocity of constituent ν can be obtained by substituting (18) into (15) and dividing through by ϕ^ν to give

$$w^\nu = w + \sum_{\forall \mu} q_{\nu\mu}\phi^\mu - D\frac{\partial}{\partial z}(\ln\phi^\nu), \tag{21}$$

where $q_{\nu\mu}$ is the maximum segregation velocity of phase ν relative to phase μ, and D is the diffusivity. These are defined as

$$q_{\nu\mu} = B_{\nu\mu}(g/c)\cos\zeta, \quad D = d/c, \tag{22}$$

respectively. In the absence of diffusion, the segregation stops whenever the particles are in a pure phase, since $\phi^\nu = 1$ necessarily implies that $\phi^\mu = 0$ for $\mu \neq \nu$.

It is convenient to introduce non-dimensional variables using the scalings

$$\left.\begin{array}{c} x = L\tilde{x}, \quad z = H\hat{z}, \quad (u,v) = U(\hat{u},\hat{v}), \\ (w,w^\nu) = (HU/L)(\hat{w},\hat{w}^\nu), \quad t = (L/U)\hat{t}, \end{array}\right\} \quad (23)$$

where L is a typical downstream length scale, H is a typical thickness and U is a typical downstream velocity magnitude. Substituting the scalings into equation (21) implies that the non-dimensional normal velocity of constituent ν is

$$w^\nu = w + \sum_{\forall \mu} S_{\nu\mu}\phi^\mu - D_r \frac{\partial}{\partial z}(\ln \phi^\nu), \quad (24)$$

where the hats have been dropped for simplicity. The non-dimensional segregation rates $S_{\nu\mu}$ and the non-dimensional diffusion coefficient are

$$S_{\nu\mu} = \frac{L}{HU} q_{\nu\mu}, \quad D_r = \frac{DL}{H^2 U}. \quad (25)$$

The matrix $\mathbf{S}$ formed by the segregation coefficients $S_{\nu\mu}$ is also antisymmetric, since it is proportional to $\mathbf{B}$ through equations (22) and (25). The segregation rate $S_{\nu\mu}$ is positive if constituent ν is larger than constituent μ. An evolution equation for the concentration of each phase ν is obtained by substituting the normal velocity (24) into the non-dimensionalized mass balance equation (5) with the downstream and cross stream velocity given by (14). The non-dimensional segregation remixing equation for phase ν is therefore

$$\frac{\partial \phi^\nu}{\partial t} + \nabla \cdot (\phi^\nu \mathbf{u}) = \frac{\partial F^\nu}{\partial z}, \quad (26)$$

where the flux in the normal direction

$$F^\nu = -\sum_{\forall \mu} S_{\nu\mu}\phi^\nu \phi^\mu + D_r \frac{\partial \phi^\nu}{\partial z}, \quad (27)$$

accounts for the segregation and diffusion of the particles. For a given incompressible bulk velocity field $\mathbf{u}$, equation (26) must be solved subject to no flux conditions at the surface and the base of the avalanche

$$F^\nu = 0, \quad \text{at} \quad z = s(x,y,t), \quad \& \quad z = b(x,y,t). \quad (28)$$

Equation (26) has been carefully constructed to ensure that when it is summed over all constituents it yields the bulk incompressibility condition

$$\nabla \cdot \mathbf{u} = 0. \quad (29)$$

This together with the lithostatic pressure distribution (9), are the key assumptions underlying most models for granular avalanches and geophysical mass flows [e.g 21, 22, 23, 24, 25, 26, 27, 28]. The bulk three-dimensional velocity field $\mathbf{u}$ may be reconstructed from depth-averaged avalanche models [e.g. 29], or it may also be computed directly using the $\mu(I)$ rheology [30].

Segregation in three-component mixtures

For a three constituent mixture, composed of large, medium and small particles, which will be denoted by the constituent letters $\nu = l, m, s$, there are three independent positive segregation rates S_{lm}, S_{ls} and S_{ms}. The antisymmetry property implies that the remaining segregation coefficients are $S_{ml} = -S_{lm}$, $S_{sl} = -S_{ls}$ and $S_{sm} = -S_{ms}$. For a three-constituent mixture the general theory yields three equations

$$\frac{\partial \phi^l}{\partial t} + \nabla \cdot (\phi^l \mathbf{u}) = \frac{\partial F^l}{\partial z}, \quad (30)$$

$$\frac{\partial \phi^m}{\partial t} + \nabla \cdot (\phi^m \mathbf{u}) = \frac{\partial F^m}{\partial z}, \quad (31)$$

$$\frac{\partial \phi^s}{\partial t} + \nabla \cdot (\phi^s \mathbf{u}) = \frac{\partial F^s}{\partial z}, \quad (32)$$

where the normal fluxes

$$F^l = -S_{lm}\phi^l\phi^m - S_{ls}\phi^l\phi^s + D_r\frac{\partial \phi^l}{\partial z}, \quad (33)$$

$$F^m = S_{lm}\phi^m\phi^l - S_{ms}\phi^m\phi^s + D_r\frac{\partial \phi^m}{\partial z}, \quad (34)$$

$$F^s = S_{ls}\phi^s\phi^l + S_{ms}\phi^s\phi^m + D_r\frac{\partial \phi^s}{\partial z}. \quad (35)$$

The summation condition (2) implies that

$$\phi^l + \phi^m + \phi^s = 1, \quad (36)$$

which allows one of the three equations (33)–(35) to be eliminated. For instance, substituting for ϕ^m in (33) and (35) yields two coupled equations for the large and small particle concentrations

$$\frac{\partial \phi^l}{\partial t} + \nabla \cdot (\phi^l \mathbf{u}) = \frac{\partial F^l}{\partial z}, \quad (37)$$

$$\frac{\partial \phi^s}{\partial t} + \nabla \cdot (\phi^s \mathbf{u}) = \frac{\partial F^s}{\partial z}, \quad (38)$$

where the normal fluxes are

$$F^l = -S_{lm}\phi^l(1-\phi^l-\phi^s) - S_{ls}\phi^l\phi^s + D_r\frac{\partial \phi^l}{\partial z}, \quad (39)$$

$$F^s = S_{ls}\phi^s\phi^l + S_{ms}\phi^s(1-\phi^l-\phi^s) + D_r\frac{\partial \phi^s}{\partial z}. \quad (40)$$

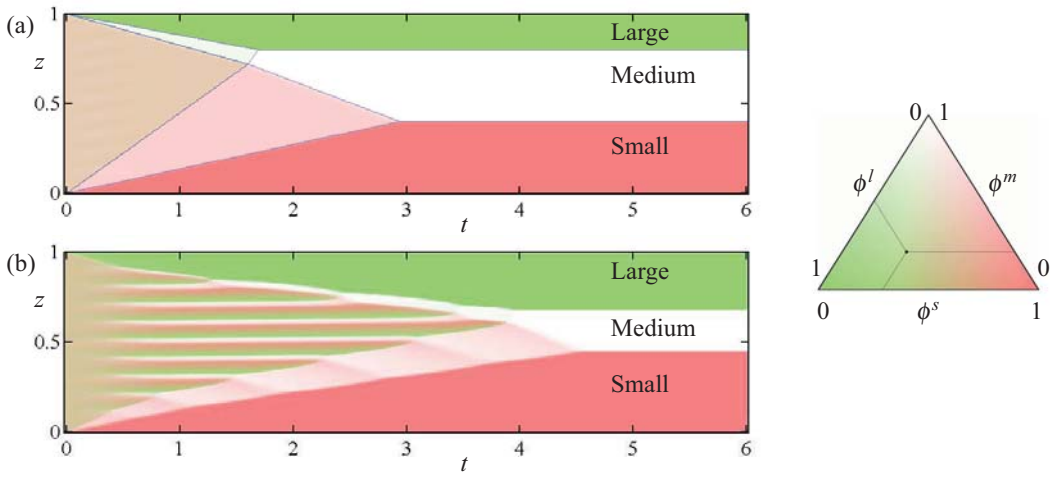

FIGURE 3. Two time-dependent simulations of the particle concentration in a three-phase mixture, showing that the segregation may be (a) stable or (b) unstable. Both simulations assume $S_{ls} = 1/8$, $S_{lm} = 1$, $S_{ms} = 3/8$ and $D_r = 10^{-3}$ and there is a small sinusoidal perturbation to the homogeneous initial condition. In (a) the inflow concentrations are $\phi_0^l = 0.2$, $\phi_0^m = 0.4$, $\phi_0^s = 0.4$ and in (b) $\phi_0^l = 0.32$, $\phi_0^m = 0.23$, $\phi_0^s = 0.45$. Each panel shows two contour plots, one for the concentration of large particles in green and one for small particles in red, which are overlaid with opacity 50%. The concentration can be determined by the triangular contour scale on the right. The solid blue lines in panel (a) show the position of concentration shocks from an exact solution to the homogeneous inflow problem in the absence of diffusion.

This represents a system of two coupled parabolic equations for the large and small particle concentrations, which can be solved using standard Galerkin finite elements methods e.g. `pdepe` in matlab.

One might expect that the larger the size ratio between the particles the larger the segregation rate. However the experiments of Golick and Daniels [31] suggest that the maximum rates may occur close to a size ratio of two. If this is the case, it is possible for the segregation rate of the large and medium particles and the medium and small particles to both be larger than the rate for large and small, i.e. $S_{ls} < S_{lm}$ and $S_{ls} < S_{ms}$. This can lead to some interesting effects as shown in figure 3. For some homogeneous initial conditions the solution is (a) stable and the grains separate out into sharply segregated inversely graded layers, but for other initial conditions (b) a small perturbation can grow rapidly to create a saw tooth segregation pattern, before the grains separate into two-component sub-mixtures and the instability decays. In the limit of no diffusion the instability is of Hadamard type [32, 33], which indicates that diffusion is needed to maintain well-posedness.

It is also possible to compute steady-state solutions for the evolution of the inflow concentration down a chute as shown in figure (4). When (a) all the grains participate in the segregation they eventually develop a *reverse distribution grading* in which the entire grain size population coarsens upwards, but if (b) the fines do not segregate then a *reverse coarse tail distribution* develops in which the large and medium grains inverse grade and the small particles are found everywhere. Note that the fully developed steady-state solution shown in figure 4(a) is very close to the distribution in the experimental avalanche shown in figure 2, which indicates that the theory is capable of making useful predictions.

Segregation in two-component mixtures

It is also useful to relate the multi-component theory to the case of a two-component mixture of large and small particles, which will be referred to by the constituent letters l and s. There is a single positive segregation rate S_{ls}, since $S_{sl} = -S_{ls}$. The general theory (26) yields two segregation equations for the large and small particles

$$\frac{\partial \phi^l}{\partial t} + \nabla \cdot (\phi^l \mathbf{u}) = \frac{\partial F^l}{\partial z}, \tag{41}$$

$$\frac{\partial \phi^s}{\partial t} + \nabla \cdot (\phi^s \mathbf{u}) - \frac{\partial F^s}{\partial z}, \tag{42}$$

where the normal fluxes are

$$F^l = -S_{ls}\phi^l\phi^s + D_r\frac{\partial \phi^l}{\partial z}, \tag{43}$$

$$F^s = S_{ls}\phi^s\phi^l + D_r\frac{\partial \phi^s}{\partial z}, \tag{44}$$

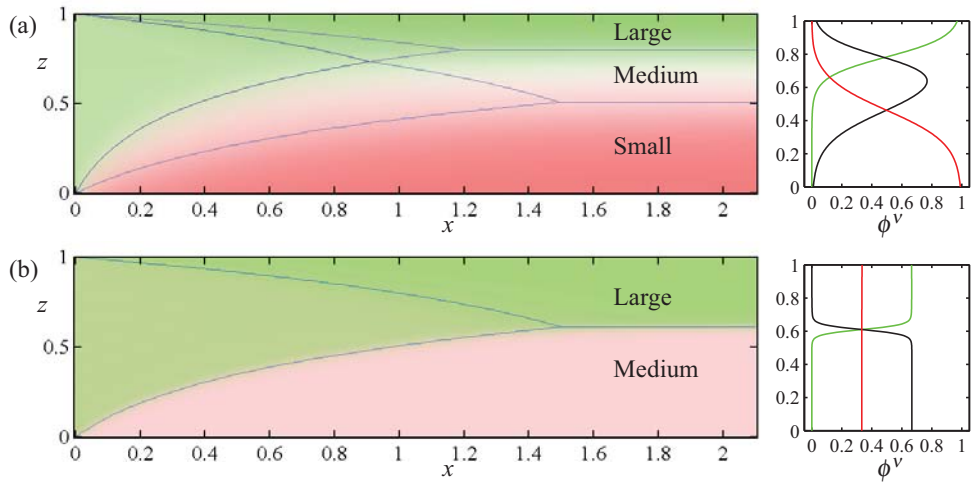

FIGURE 4. Steady-state solutions for the segregation of large, medium and small particles showing the formation of (a) reverse distribution grading and (b) reverse coarse tail grading. The avalanche is assumed to be of unit depth with downslope velocity profile $u = \beta \exp(\beta z)/(\exp(\beta) - 1)$ with $\beta = 3.3$. In panel (a) $S_{ls} = 1$, $S_{lm} = 0.8$, $S_{ms} = 0.5$, $D_r = 0.05$, and the inflow concentrations $\phi_0^l = 1/2$, $\phi_0^m = 1/3$, $\phi_0^s = 1/6$. In panel (b) $S_{ls} = 0$, $S_{lm} = 1$, $S_{ms} = 0$, $D_r = 0.01$, and the inflow concentrations are $\phi_0^l = 1/2$, $\phi_0^m = 1/6$, $\phi_0^s = 1/3$. In the lefthand concentration plots the same contour scale as figure 3 is used. On the right the final concentrations as a function of height are shown for large (green line), small (red line) and medium (black line) grains. The solid blue lines in the lefthand plots show the position of concentration shocks from an exact solution to the homogeneous inflow problem in the absence of diffusion.

and the summation condition (2) is

$$\phi^l + \phi^s = 1. \tag{45}$$

Gray and Thornton [19] decided to use (45) to substitute for the large particle concentration. The resulting segregation equation for the concentration of the small particles can therefore be written as

$$\frac{\partial \phi^s}{\partial t} + \nabla \cdot (\phi^s \mathbf{u}) - \frac{\partial}{\partial z}\left(S_{ls}\phi^s(1-\phi^s)\right) = \frac{\partial}{\partial z}\left(D_r \frac{\partial \phi^s}{\partial z}\right). \tag{46}$$

Bridgwater et al. [34] were probably the first to write down a time-dependent version of this equation, which was based on the idea of the competition between percolation and diffusion. Savage and Lun [13] used statistical mechanics to derive a theory for kinetic sieving and squeeze expulsion, which to leading order yielded the same structure for the segregation term [19], but neglected diffusive effects. Vallance and Savage [14] showed that solutions to this theory were consistent with experiments on an inclined chute. Dolgunin and Ukolov [35] also wrote down this equation, based on the simple insight that the segregation flux $-S_{ls}\phi^s(1-\phi^s)$ must shut off, when there are either all small particles, or all large ones. The equation is closely related to Burgers' equation, which Gray and Chugunov [20] exploited, by means of the Cole-Hopf transformation, to construct exact solutions for time-dependent segregation with diffusion. Wiederseiner et al. [36] have obtained excellent agreement between the diffuse theory and detailed experimental data collected at the side wall of a chute. They showed that typical Peclet numbers $Pe = Sr/Dr$ are of the order to 10-20. This equation has also proved useful in understanding segregation due to density differences between the particles [37, 38].

In the absence of diffusion it is possible to construct solutions by the method of characteristics. A range of two-dimensional steady-state [19, 39] and time-dependent [40, 41, 42] exact solutions have been constructed. A highlight of the theory is its ability to predict the formation of breaking size segregation waves, which form whenever small particles are sheared over large ones [43, 29, 44] as shown in the sequence of images in figure 5. The avalanche is initially inversely graded with a sharp interface between the large (green) particles and small (pink) grains that decreases linearly with increasing downslope distance x. Since the downslope bulk velocity is larger at the surface than at the base, the interface steepens with increasing time and breaks at $t = 1$. A layer of small particles is then sheared over the large grains, which are then squeezed up into faster moving parts of the flow and allow the small ones percolate down into slower moving regions. The net result is a continuously breaking particle-size segregation wave that allows large and small particles to recirculate in the flow. This is particularly important in the geophysical context, where they are fundamen-

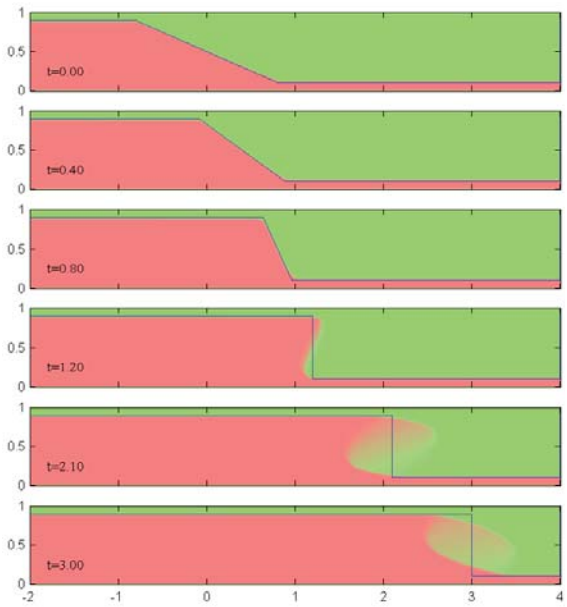

FIGURE 5. A series of (x,z) plots showing the formation of a breaking size segregation wave in a bi-disperse unit depth avalanche at a sequence of times. The particle concentration is shown using the same contour scale as figure 3. Initially the avalanche is sharply inversely graded with an upstream concentration shock $\eta_{up} = 0.9$ that is connected to the downstream interface $\eta_{down} = 0.1$ by a linear transition in the region $-0.8 < x < 0.8$. The velocity field is simple shear ($\alpha = 0$) and the segregation rate $S_{ls} = 1$. The interface position from the depth-averaged theory is plotted in blue.

tal to the formation of bouldery flow fronts [29, 45], lateral instabilities and the spontaneous formation of coarse rich levees that channelize the flow and enhance run-out [46, 47, 48, 49, 50, 51, 52, 53, 54, 55].

A depth-averaged segregation model

Solving the full size segregation equations in evolving three-dimensional flows still represents a considerable challenge. An alternative approach is to integrate the segregation equation through the avalanche depth, to derive a depth-averaged segregation equation. This fits naturally into the depth-averaged framework of current avalanches models. For instance, neglecting cross-slope terms in (46) and using Leibniz' integral theorem, together with the surface and basal kinematic and no flux (28) conditions, implies

$$\frac{\partial}{\partial t}(h\bar{\phi}) + \frac{\partial}{\partial x}(h\overline{\phi u}) = 0, \tag{47}$$

where the depth-averaged concentration of small particles and the depth integrated flux of small particles are

$$\bar{\phi} = \frac{1}{h}\int_b^s \phi^s \, dz, \quad \text{and} \quad \overline{\phi u} = \frac{1}{h}\int_b^s \phi^s u \, dz. \tag{48}$$

It is possible to evaluate the two integrals in (48) by assuming that the avalanche is sharply inversely graded with concentration distribution

$$\phi^s = \begin{cases} 0 & l \le z \le s, \\ 1 & b \le z \le l, \end{cases} \tag{49}$$

and that the downslope velocity is linear with depth

$$u = \alpha\bar{u} + 2(1-\alpha)\bar{u}\left(\frac{z-b}{h}\right), \quad 0 \le \alpha \le 1. \tag{50}$$

where $\bar{u}$ is the depth-averaged downslope velocity and $z = b(x,t)$ is the height of the topography. The parameter α allows the velocity profile to vary from plug-flow ($\alpha = 1$), to simple shear ($\alpha = 0$), and linear shear with basal slip for intermediate values. With these assumptions it follows that

$$h\bar{\phi} = l - b = \eta, \tag{51}$$

$$h\overline{\phi u} = \eta\bar{u} - (1-\alpha)\bar{u}\eta\left(1 - \frac{\eta}{h}\right). \tag{52}$$

Substituting (51) and (52) into (47) yields an important new equation for the depth of small particles, η,

$$\frac{\partial \eta}{\partial t} + \frac{\partial}{\partial x}(\eta\bar{u}) - \frac{\partial}{\partial x}\left((1-\alpha)\bar{u}\eta\left(1 - \frac{\eta}{h}\right)\right) = 0. \tag{53}$$

This equation essentially tracks the evolving position of the concentration shock between the inversely graded layers of large and small particles. By using (51) it is also possible to write (53) as

$$\frac{\partial}{\partial t}(h\bar{\phi}) + \frac{\partial}{\partial x}(h\bar{u}\bar{\phi}) - \frac{\partial}{\partial x}\left((1-\alpha)h\bar{u}\bar{\phi}\left(1-\bar{\phi}\right)\right) = 0, \tag{54}$$

which is remarkably similar to the segregation equation (46) from which it is derived. In particular the form of the segregation term $\phi^s(1-\phi^s)$ in (46) is very similar to the term $\phi(1-\phi)$ in the (54), which immediately tells us that the depth-averaged equation also segregates particles, but laterally rather than vertically. Indeed, Gray and Kokelaar [45] called this the large particle transport equation, because it preferentially transports large particles towards the avalanche front, and allows them to recirculate there. In the breaking size segregation problem shown in figure 5, the two theories are identical up until the wave breaks at $t = 1$, and then a shock in the interface height forms, which moves at the same speed as the wave. This equation therefore opens up the realistic possibility of coupling the basal friction of the bulk flow to the evolving particle size distribution, to model the subtle *segregation-mobility* feedback effects that lead to the formation of coarse particle rich levees [49, 54] and flow fingering [47, 48, 55].

ACKNOWLEDGMENTS

This research was supported by EPSRC grants EP/K00428X/1, EP/I019189/1 & GR/S50052/01, as well as NERC grants NE/K003011/1, NER/A/S/2003/00439 and NE/E003206/1.

REFERENCES

1. B. A. Wills, *Mineral Processing Technology*, Pergamon, 1979.
2. J. R. Johanson, *Chem. Eng.* pp. 183–188 (1978).
3. S. C. Williams, *Powder Technol.* **2**, 13–20 (1968).
4. J. Bridgwater, *Powder Technol.* **15**, 215Ű236 (1976).
5. J. A. Drahun, and J. Bridgwater, *Powder Technol.* **36**, 39–53 (1983).
6. R. A. Bagnold, *P. Roy. Soc. Lond. A* **225**, 49–63 (1954).
7. G. V. Middleton, "Experimental studies related to problems of flysch sedimentation," in *Flysch Sedimentology in North America*, edited by J. Lajoie, Business and Economics Science Ltd, Toronto, 1970, pp. 253–272.
8. J. J. McCarthy, *Powder Technol.* **192**, 137–142 (2009).
9. A. M. Scott, and J. Bridgwater, *Industrial & Engineering Chemistry Fundamentals* **14**, 22–27 (1975).
10. D. Schulze, *Powders and Bulk Solids*, Springer Berlin Heidelberg, 2008.
11. E. E. Ehrichs, H. M. Jaeger, G. S. Karczmar, J. B. Knight, V. Y. Kuperman, and S. R. . Nagel, *Science* **267**, 1632–1634 (1995).
12. M. Schröter, S. Ulrich, J. Kreft, J. B. Swift, and H. L. Swinney, *Phys. Rev. E* **74**, 011307 (2006).
13. S. B. Savage, and C. K. K. Lun, *J. Fluid Mech.* **189**, 311–335 (1988).
14. J. W. Vallance, and S. B. Savage, "Particle segregation in granular flows down chutes," in *IUTAM Symposium on segregation in granular materials*, edited by A. D. Rosato, and D. L. Blackmore, Kluwer, 2000.
15. A. Rosato, K. J. Strandburg, F. Prinz, and R. H. Swendsen, *Phys. Rev. Lett.* **58**, 1038–1040 (1987).
16. J. M. N. T. Gray, and C. Ancey, *J. Fluid Mech.* **678**, 535–588 (2011).
17. C. Truesdell, *Rational Thermodynamics*, Springer, 1984.
18. L. W. Morland, *Surveys in Geophysics* **13**, 209–268 (1992).
19. J. M. N. T. Gray, and A. R. Thornton, *Proc. Roy. Soc. A* **461**, 1447–1473 (2005).
20. J. M. N. T. Gray, and V. A. Chugunov, *J. Fluid Mech.* **569**, 365–398 (2006).
21. S. S. Grigorian, M. E. Eglit, and I. L. Iakimov, *Snow, Avalanches & Glaciers. Tr. Vysokogornogo Geofizich Inst* **12**, 104–113 (1967).
22. S. B. Savage, and K. Hutter, *J. Fluid Mech.* **199**, 177–215 (1989).
23. R. M. Iverson, *Rev. Geophys.* **35**, 245–296 (1997).
24. J. M. N. T. Gray, M. Wieland, and K. Hutter, *Proc. Roy. Soc. A* **455**, 1841–1874 (1999).
25. R. M. Iverson, and R. P. Denlinger, *J. Geophys. Res.* **106**, 553–566 (2001).
26. J. M. N. T. Gray, Y. C. Tai, and S. Noelle, *J. Fluid Mech.* **491**, 161–181 (2003).
27. A. Mangeney, F. Bouchut, N. Thomas, J. P. Vilotte, and M. O. Bristeau, *J. Geophys. Res.* **112**, F02017 (2007).
28. X. Cui, and J. M. N. T. Gray, *J. Fluid Mech.* **720**, 314–337 (2013).
29. J. M. N. T. Gray, and C. Ancey, *J. Fluid Mech.* **629**, 387–423 (2009).
30. P. Jop, Y. Forterre, and O. Pouliquen, *Nature* **44**, 727–730 (2006).
31. L. A. Golick, and K. E. Daniels, *Phys. Rev. E* **80**, 042301 (2009).
32. D. D. Joseph, and J. C. Saut, *Theoretical and Computational Fluid Dynamics* **1**, 191–227 (1990).
33. J. D. Goddard, *Ann. Rev. Fluid Mech.* **35**, 113–133 (2003).
34. J. Bridgwater, W. Foo, and D. Stephens, *Powder Technol.* **41**, 147 (1985).
35. V. N. Dolgunin, and A. A. Ukolov, *Powder Technol.* **83**, 95–103 (1995).
36. S. Wiederseiner, N. Andreini, G. Epely-Chauvin, G. Moser, M. Monnereau, J. M. N. T. Gray, and C. Ancey, *Phys. Fluids* **23**, 013301 (2011).
37. D. V. Khakhar, J. J. McCarthy, and J. M. Ottino, *Chaos* **9**, 594–610 (1999).
38. A. Tripathi, and D. V. Khakhar, *J. Fluid Mech.* **717**, 643–669 (2013).
39. A. R. Thornton, J. M. N. T. Gray, and A. J. Hogg, *J. Fluid Mech.* **550**, 1–25 (2006).
40. J. M. N. T. Gray, M. Shearer, and A. R. Thornton, *Proc. Roy. Soc. A* **462**, 947–972 (2006).
41. M. Shearer, J. M. N. T. Gray, and A. R. Thornton, *Eur. J. App. Math.* **19**, 61–86 (2008).
42. L. B. H. May, L. A. Golick, K. C. Phillips, M. Shearer, and K. E. Daniels, *Phys. Rev. E* **81**, 051301 (2010).
43. A. R. Thornton, and J. M. N. T. Gray, *J. Fluid Mech.* **596**, 261–284 (2008).
44. M. Shearer, and N. Giffen, *Discrete & Continuous Dyn. Sys.* **27**, 693–714 (2010).
45. J. M. N. T. Gray, and B. P. Kokelaar, *J. Fluid Mech.* **652**, 105–137 (2010).
46. T. C. Pierson, "Flow behavior of channelized debris flows, Mount St. Helens, Washington," in *Hillslope Processes*, edited by A. D. Abrahams, Allen and Unwin, Winchester, Mass., 1986, pp. 269–296.
47. O. Pouliquen, J. Delour, and S. B. Savage, *Nature* **386**, 816–817 (1997).
48. O. Pouliquen, and J. W. Vallance, *Chaos* **9**, 621–630 (1999).
49. R. M. Iverson, and J. W. Vallance, *Geology* **29**, 115–118 (2001).
50. G. Félix, and N. Thomas, *Earth & Planetary Sci. Lett.* **221**, 197–213 (2004).
51. C. Goujon, B. Dalloz-Dubrujeaud, and N. Thomas, *Eur. Phys. J. E* **23**, 199–215 (2007).
52. R. M. Iverson, M. Logan, R. G. LaHusen, and M. Berti, *J. Geophys. Res.* **115**, F03005 (2010).
53. B. Cagnoli, and G. P. Romano, *J. Volcan. Geotherm. Res.* **193**, 18–24 (2010).
54. C. G. Johnson, B. P. Kokelaar, R. M. Iverson, M. Logan, R. G. LaHusen, and J. M. N. T. Gray, *J. Geophys. Res.* **117**, F01032 (2012).
55. M. J. Woodhouse, A. R. Thornton, C. G. Johnson, B. P. Kokelaar, and J. M. N. T. Gray, *J. Fluid Mech.* **709**, 543–580 (2012).